ELSEVIER

Agricultural and Forest Meteorology 79 (1996) 113–130

AGRICULTURAL AND FOREST METEOROLOGY

Seasonal variabilities in the distribution of the microclimatic factors and evapotranspiration in a shortgrass steppe

Romelito L. Lapitan [a,*], William J. Parton [b]

[a] *Great Plains Systems Research, USDA–ARS–NPA, P.O. Box E, 301 South Howes St., Fort Collins, CO 80526, USA*

[b] *Natural Resource Ecology Laboratory, Colorado State University, Fort Collins, CO 80523, USA*

Received 6 June 1994; accepted 8 June 1995

Abstract

Ecosystem models designed to simulate the long-term dynamics of soil–vegetation–atmosphere interactions require information on the properties of the land surface and the temporal pattern of the microclimate variables. This paper describes the seasonal distributions of microclimatic factors in a semi-arid shortgrass steppe and a potential method for estimating evapotranspiration in sparse vegetation. The shortgrass steppe is located in the piedmont of north–central Colorado. Microclimate measurements were taken between 1986 and 1989. Precipitation showed wide variability between the years and could significantly account for the seasonal differences in growth and biomass yield of the native vegetation. Small (0.5 cm or less) precipitation (rain and/or dew) events, determined from the positive increments in hourly lysimeter measurements, contribute 8–10% to the total annual precipitation at the site. The total net radiation (R_n) was found to be 47% of the total incident solar radiation. The ratio of surface soil heat flux to R_n (G_s/R_n) was found uniformly equal to 0.167 during the vegetated season (April–October). Midday sensible heat flux (H) was found to be linearly related to the difference between the temperatures of the soil measured at 0.025 m depth and the air above the canopy. The ratio of H and R_n taken at midday was found to be linearly proportional to the ratio of the daily totals of H and R_n. A method for estimating daily evapotranspiration (ET_{day}) based on the energy balance approach was developed. This method was found suitable for estimating ET_{day} in the shortgrass steppe under high soil moisture conditions and/or on days following rainfall. For potential application of this method of estimating ET_{day} to dry soil conditions, integration of plant transpiration controls into the ET_{day} equation is suggested.

* Corresponding author.

Elsevier Science B.V.
SSDI 0166-3542(95)02272-4

1. Introduction

Ecosystems models linked to large-scale climate models are used to simulate long-term dynamics and directional changes in vegetation pattern, biogeochemical cycling processes, and their potential feedback effects on climate (Dickinson et al., 1986; Sellers et al., 1986). Basic and critical inputs to these models are information about the surface (soil and vegetation) properties, dynamics of surface energy exchange, and the temporal pattern of microclimate variables that would allow parameterization of the soil–vegetation–atmosphere interactions from the local scale to regional scale. As part of the US-IBP Grassland Biome Project, long-term micrometeorological measurements at a shortgrass steppe located in the piedmont of north–central Colorado were made primarily to generate this information. These data can also be used to better understand the climatic controls on the structure and composition of the grassland vegetation (Sala and Lauenroth, 1982; Sala and Lauenroth, 1984), rates of production and turnover of soil organic residues (Parton et al., 1987; Parton et al., 1988), and biogeochemical cycling of carbon and nitrogen nutrients (Schimel et al., 1985; Schimel and Parton, 1986; Parton et al., 1988) in a relatively unperturbed grassland ecosystem. The objective of this paper is to describe the seasonal pattern of microclimate variables important in deriving information on surface roughness, evapotranspiration, and partitioning of radiative heat energy in the shortgrass steppe. An understanding of the extreme fluctuations and consistent patterns in the distribution of these microclimate variables may provide answers to why some dominant plant species have almost reached equilibrium in this semi-arid environment. The data have been presented in quantitatively descriptive forms for a better characterization of the temporal dynamics of the microclimate in a shortgrass steppe.

2. Site description and instrumentation

The Long-Term Ecological Research (LTER) site is situated within the Pawnee National Grassland in north–central Colorado (40°49′N, 104°45′W). The site is managed by the USDA–ARS Central Plains Experimental Range (CPER) and consists of gently rolling terrain with an average elevation of 1650 m above mean sea-level. Soil type is Vona fine sandy loam (coarse-loamy, mixed mesic; Ustollic Haplargid) characterized by a weakly developed B horizon and a solum depth not exceeding 0.30 m. The soil consisted of 3% organic matter, 97% minerals, and has an average bulk density of $1.38 \times 10^3\ \mathrm{kg\,m^{-3}}$ (Van Haveren and Galbraith, 1971; Schimel et al., 1985). Of the native vegetation at the Pawnee site described by Klipple and Costello (1960), 17 major perennial and annual plant species have been identified at the CPER. Blue grama grass (*Bouteloua gracilis* (H.B.K.) Lag) was found to be the dominant grass species (Lauenroth and Dodd, 1978) in the shortgrass steppe.

The climate pattern at the CPER is typical of mid-continental areas, characterized by high solar radiation, strong winds, and wide seasonal variations in precipitation, atmospheric humidity and temperature. Approximately 25% of the total annual precipita-

tion is contributed by snowfall and 65% by rainfall. Annual rainfall for a dry year (1986) was 17.5 cm and for a wet year (1988) was 28.2 cm.

The LTER site is equipped with an automated weather station. Hourly microclimate data were recorded using a 21X datalogger (Campbell Scientific, Logan, UT). Data taken from 1986 to 1989 were used in this study. The total incoming global solar radiation (S_t) was measured using a Li-Cor 200 SB pyranometer (Li-Cor, Lincoln, NE). A double-dome Fritschen-type net radiometer (Micromet Instruments, Seattle, WA), wet-bulb, and dry-bulb thermometers were placed 1 m above the soil surface to measure net radiation (R_n), wet-bulb, and dry-bulb air temperatures, respectively. Wind direction (Met One, Grants Pass, OR) was measured at 4 m above the soil surface. Profile measurements of wind speed (Met One, Grants Pass, OR) were taken at 1, 2, and 4 m heights. Profile measurements of soil temperature were obtained at 0.025, 0.04, 0.10, 0.20 and 0.50 m depths using copper–constantan thermocouples. Soil water loss by evapotranspiration was determined from the hourly differences in the values recorded from weighing-lysimeter (Armijo et al., 1972) measurements.

Diurnal and seasonal changes in precipitation were determined using the lysimeter and tipping-bucket raingauge measurements. No irrigation was provided at the CPER site and water inputs were primarily from snowfall, rainfall or night-time condensation of water vapor. Rainfall measurements taken from a Standard Weather Station located 50 m from our site were used to further check our precipitation measurements. These data are stored at the National Atmospheric Deposition Program (Fort Collins, CO). Profile measurements of soil moisture inside the lysimeter were made at 2 week intervals using a nuclear soil moisture gauge (Troxler, Research Triangle Park, NC).

The shortwave albedo of the surface, composed of the soil, green vegetation, and senesced vegetation from the previous growing season, was obtained by multiplying S_t ($MJ\,m^{-2}\,h^{-1}$) by the reflectance factors (α) shown in Fig. 1. These reflectance factors were the average of 4 years (1972–1975) of surface reflectance measurements made by W.J. Parton (unpublished data, 1975) using a downward-facing pyranometer (Kipp and Zonen, Holland) at 1 m above the surface. To completely describe the radiation regime

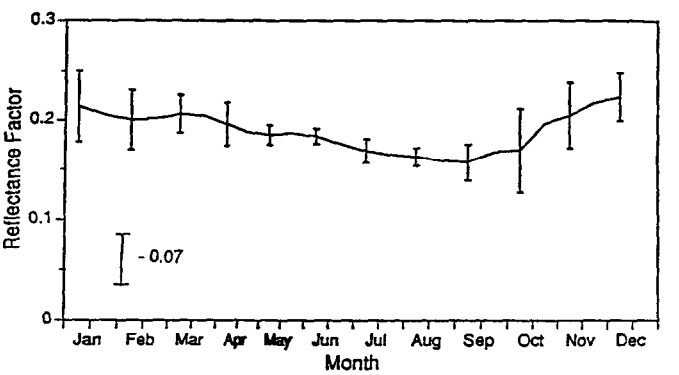

Fig. 1. Temporal variations of mean surface reflectance (fraction) of shortwave radiation taken over a shortgrass prairie, 1972–1975. Bar line represents standard error of the mean.

in the shortgrass steppe, net longwave radiation (L_n), cloudiness (F_c), and daylength (D_l) were derived from values of the other measured radiation factors. Net longwave radiation (L_n) was calculated from

$$L_n = R_n - (1 - \alpha) S_t \tag{1}$$

The fraction of sky covered by clouds, F_c, was determined from the ratio of the measured global solar radiation and solar irradiance under a standard clear sky. For a standard clear sky, solar irradiance is the sum of direct (S_d) and diffuse (S_f) radiation, and has been described by List (1971) and Dougniaux (1976) as

$$S_d = S_o a^m \cos\theta \tag{2}$$

$$S_f = 7.61 \times 10^{-3} \int_{\theta}^{\frac{\pi}{2}} \int_{\phi}^{2\pi} L(\theta', \phi') \cos\theta \cos\phi \, d\theta \, d\phi \tag{3}$$

where S_o is the extraterrestrial radiation (4.9 MJ m^{-2} h^{-1}), a is the atmospheric transmission coefficient taken as 0.84 for clear days, m is the pressure-corrected optical air mass (Kasten, 1966), and $L(\theta', \phi')$ is the luminance distribution of a clear sky at θ' (elevation) and ϕ' (azimuth) of the spherical zone of the sky. The solar zenith (θ) and azimuth (ϕ) angles were calculated from Walraven (1978). Daylength (D_l; h day^{-1}) was determined by curve fitting the total daylight period (h) with day of the year ($r^2 = 0.96$; root mean square error (RMSE) = 0.41), and expressed as

$$D_l = 2.05 + 5.65 \left\{ 1 + \sin^2 \left[\frac{\pi (\text{Day} + 10)}{365} \right] \right\} \tag{4}$$

where $\pi = 3.14159$ and Day is the number Jan 1 = 1 (Johnson and Thornley, 1983).

The physical and operating conditions of the instruments were checked consistently at 2 week intervals. The net radiometer was calibrated every year, whereas the pyranometer and wind vector instruments were calibrated once during the 1986–1989 period. Also, field site calibrations of the net radiometer were made by comparisons with the Swissteco (Swissteco, Switzerland) and Fritschen Q*5 net (Micromet Instruments, Seattle, WA) radiometers.

Surface soil heat flux, G_s (MJ m^{-2} h^{-1}) was calculated using the equation

$$G_s = G_{10} + \Delta z C_s \left(\frac{\Delta T_m}{\Delta t} \right) \tag{5}$$

where G_{10} is heat flux density measured by heat-flow transducer plates at 0.10 m (Δz) depth in the soil, $\Delta z C_s$ ($\Delta T_m / \Delta t$) refers to the change in the energy stored above the transducer plates, T_m is the average soil temperature (°C) above 0.10 m depth, and t is time (h). Three heat-flow transducer plates were laid out randomly around the weather station. The volumetric heat capacity (C_s) of the soil (MJ m^{-3} °C^{-1}) was calculated as

$$C_s = 0.99 + 4.19\theta_w \tag{6}$$

where θ_w is the volumetric soil water content (m^3 m^{-3}).

3. Results and discussion

3.1. Precipitation and evapotranspiration

Precipitation at the LTER site was determined from lysimeter (P_{Lys}) and tipping-bucket raingauge (P_{TB}) measurements. P_{TB} has relatively lower sensitivity than P_{Lys} and may be unreliable especially during the winter (December–March) months. However, P_{Lys} may underestimate rainfall under conditions of high solar radiation following a short rainfall event (less than 1 h duration). This is because P_{Lys} was recorded hourly and the values reflect net changes (rainfall minus evapotranspiration) within the hour. P_{TB} measurements were recorded at 15 min intervals. The magnitude of error under such cases is 0.3 cm or less, which is still less than the sensitivity of P_{TB}. The positive increments in P_{Lys} measurements were analyzed carefully to eliminate errors that may be caused by deposition of wind-blown snow, plant, and soil materials during the winter and in months with strong winds.

The monthly total distribution of precipitation of 0.5 cm or less and of more than 0.5 cm, and frequency of occurrence of precipitation events of more than 0.5 cm at the CPER are shown in Fig. 2. Of the total annual precipitation, 74% occurred between May and September. Precipitation events of 0.5 cm or less were common (80% or more) during each month of the year. During the winter months, conditions were favorable for hoar frost formation but because of the effects of wind-blown snow, positive increments

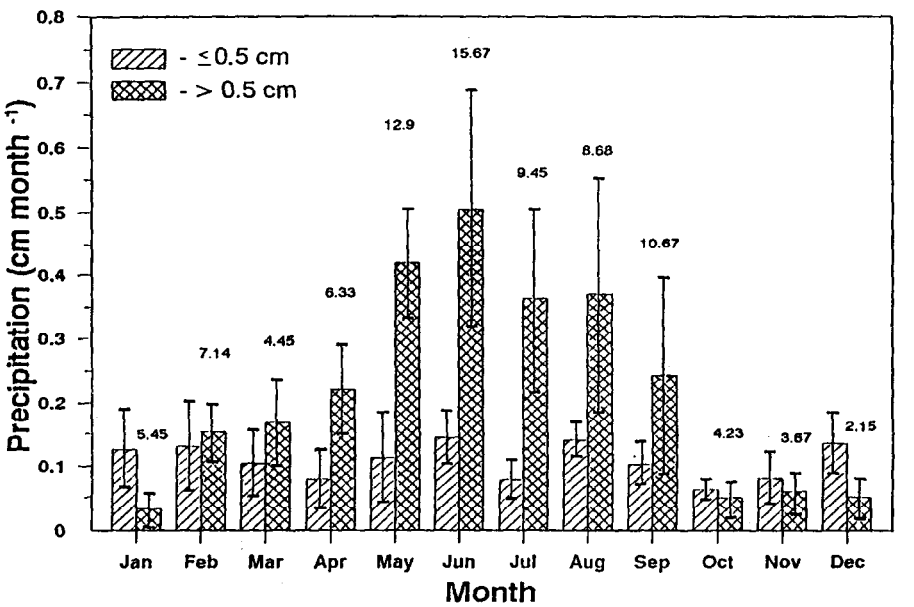

Fig. 2. Monthly total distribution of precipitation events of 0.5 cm or less and of more than 0.5 cm. The numbers above the bar for more than 0.5 cm indicate the frequency of occurrence (%) of precipitation events of more than 0.5 cm at the CPER, 1986–1989. Bar line represents standard error of the mean.

Table 1
Nocturnal microclimate measurements determining night-time condensation at the CPER, 1989

Variables	Day of year		
	1 July	17 August	3 December
Cloudiness [a] (tenths of sky)	0.1	0.2	0.2
Wind speed ($m\,s^{-1}$)	1.0	0.8	1.2
Vapor pressure (kPa)			
Actual	1.2	1.2	1.3
Saturated	1.1	1.2	1.3
Temperature (°C)			
Air	10.6	9.7	13.8
Canopy	9.2	9.1	9.8
Dewpoint	9.0	8.9	9.8
Dew formed (cm)	0.006	0.011	0.019

[a] Average of cloudiness calculated from the previous and the present day.

in P_{Lys} were difficult to attribute to this cause. Nocturnal microclimate measurements made between April and October indicated conditions favoring formation of dew (Table 1). Night-time positive increments in P_{Lys} were mainly observed between 00:00 and 05:00 h MST (Mountain Standard Time). The surface temperature and actual vapor pressure closely approached dewpoint temperature and saturation vapor pressure, respectively, during this time period. Low wind speeds (less than $2\,m\,s^{-1}$) and clear sky conditions, taken as the average F_c from two consecutive days, were also observed during this period. Precipitation events of 0.5 cm or less accounted for 8–10% of the total annual precipitation. Ecologically, these small precipitation events have been found significant in determining the structure of the plant community (Sala and Lauenroth, 1982; Sala and Lauenroth, 1984) and in influencing the biogeochemical cycling of soil nutrients (Schimel and Parton, 1986) in arid and semi-arid grassland ecosystems.

Daily evapotranspiration (ET_{day}) rates closely followed the seasonal distribution of rainfall (Fig. 3) and high rates of ET_{day} coincided with the presence of vegetation, high solar radiation, and high soil moisture. Vegetative growth starts in April, peak leaf area index is observed between May and June, and complete senescence is achieved at the end of October (Hazlett, 1992). High soil moisture content early in the season was the result of spring thawing and high rainfall. A second major recharge of soil water was consistently observed during September from 1986 to 1989.

Two drying periods were consistently observed each year. One was between the fourth week of May and second week of June; the other between the second week of August and first week of September. During these periods, mean rainfall was 0.25 cm or less, the mean volumetric fraction of soil water to 0.20 m depth was $0.1\,m^3\,m^{-3}$ or less, and ET_{day} was equal to $0.05\,cm\,day^{-1}$ or less. The September rainfall was favorable for regrowth of the native vegetation, as was observed from the upswing in leaf area index, per cent leaf nitrogen content, and green biomass during the month (unpublished data).

Precipitation of 0.5 cm or less totally evaporates within 1 h. Rainfall events of 1.0–4.3 cm recharged the soil water to soil depths of 0.60–1.20 m (Fig. 4(a)). Gravimetric soil moisture measurements of samples taken from 0 to 0.15 m soil depths following

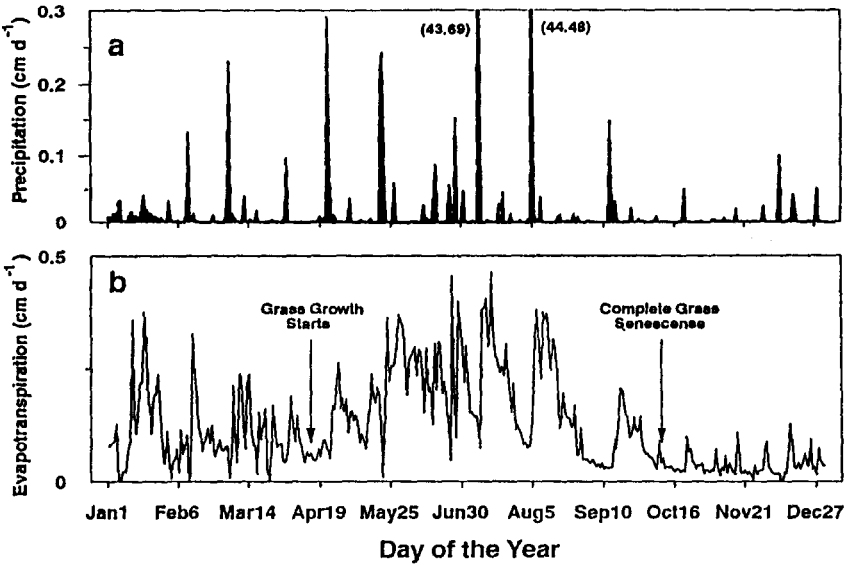

Fig. 3. Seasonal distribution (in cm day^{-1}) of (a) rainfall and (b) evapotranspiration rates at the shortgrass prairie, CPER, 1988.

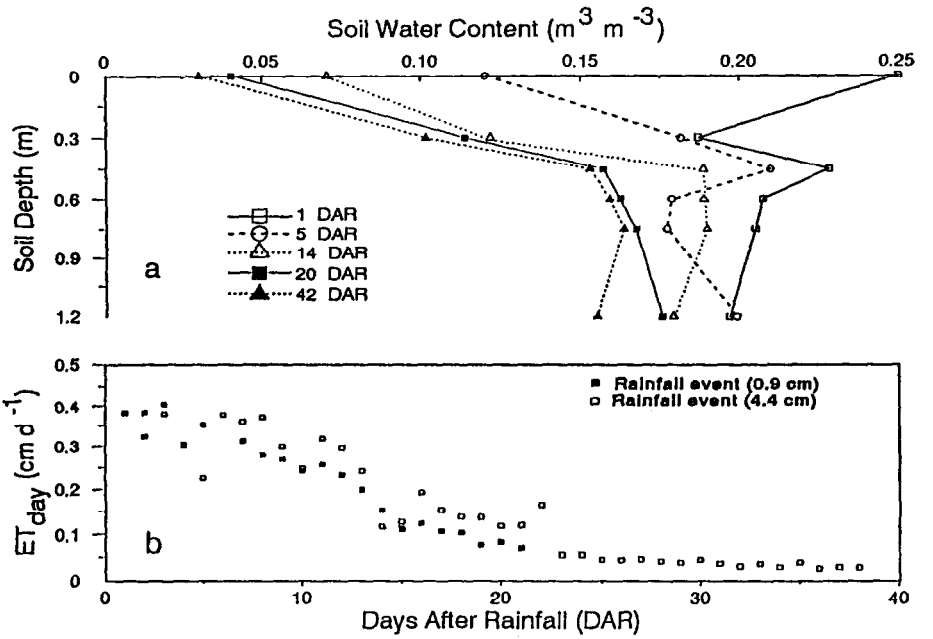

Fig. 4. Profile distributions of (a) soil water content ($m^3 m^{-3}$) on days after 4.4 cm of rainfall (DAR), and (b) temporal distributions of evapotranspiration rates (cm day^{-1}) during two wetting–drying events, CPER, 1988.

rainfall of 1.0–4.3 cm showed soil moisture levels ranging from 0.25 to 0.34 $m^3\ m^{-3}$. Soil moisture levels at depths between 0.15 and 0.90 m ranged from 0.17 to 0.23 $m^3\ m^{-3}$. ET_{day} was highest during the first 5 days following soil wetting (Fig. 4(b)). During this period, soil water loss was greatly observed at the top 0.3 m depth. During the rapid dry-down phase of the ET_{day} curve, between 5 and 20 days after rainfall, water is being drawn from deeper depths to meet the atmospheric demand for water. When ET_{day} was at its minimum rate (0.03 cm day^{-1}), the volumetric fraction of soil moisture content at 0–0.15 m depths ranged between 0.03 and 0.05 $m^3\ m^{-3}$.

3.2. Air and soil temperatures

The seasonal distributions of daily maximum and minimum air temperatures in the shortgrass steppe can be described by the empirical equation given by Johnson and Thornley (1983) as

$$T_{a(\max/\min)} = a + b\sin^2\left[\frac{\pi(\text{Day} - 24)}{365}\right] \tag{7}$$

where $a = 4.73$ and $b = 25.93$ for maximum air temperature ($r^2 = 0.91$; RMSE = 2.79), $a = -12.35$ and $b = 23.04$ for minimum air temperature ($r^2 = 0.90$; RMSE = 2.60). For the period 1986–1989, the mean daily maximum and minimum air temperatures observed during the vegetative season (April–October) were 30.84 ± 4.0°C and 8.54 ± 2.5°C, respectively.

The daily soil temperatures (T_s) measured at the surface to 0.25 m depths were consistently higher (varied between 1 and 12°C) than the daily air temperature (T_a) during the vegetative season. Conversely, the daily mean T_s was consistently lower (maximum of 20°C difference) than the daily mean T_a during the winter months. The widest variability in soil temperatures (T_s) were observed in depths close to the soil surface, as expected. Maximum T_s was consistently observed at 0.025 m depth, except during the winter months, when T_s at 0.20 m depth were 2–3°C higher than those measured at 0.025 m depth.

After a large rainfall event (4 cm or more), the temperatures along the soil profile remained similar for 3 days (Fig. 5). As the soil dries, T_s drastically increased, in effect creating a thermal gradient of 6°C or more between 0.025 and 0.20 m depths. During this rapid dry-down period, the daily temperature differences between T_s at 0.025 m depth and T_a were found to be significantly and linearly correlated ($r = 0.76$; $P \leq 0.05$) with ET_{day}. This suggests the potential use of surface soil temperature measurements for assessing soil water loss.

It should be pointed out that during the vegetative season, shading caused by the standing biomass may affect soil temperature despite the sparse plant distribution. Parton (1984) observed substantial reductions in hourly temperature variations at the soil surface under the plant canopy. He also noted a decrease of 5–15°C in daily maximum and decrease of 1–2°C in minimum soil temperatures with increase in standing biomass. Our study, however, indicated very little effect of blue grama grass canopy on the amount of radiative energy reaching and conducted into the soil. The implications of this are discussed below.

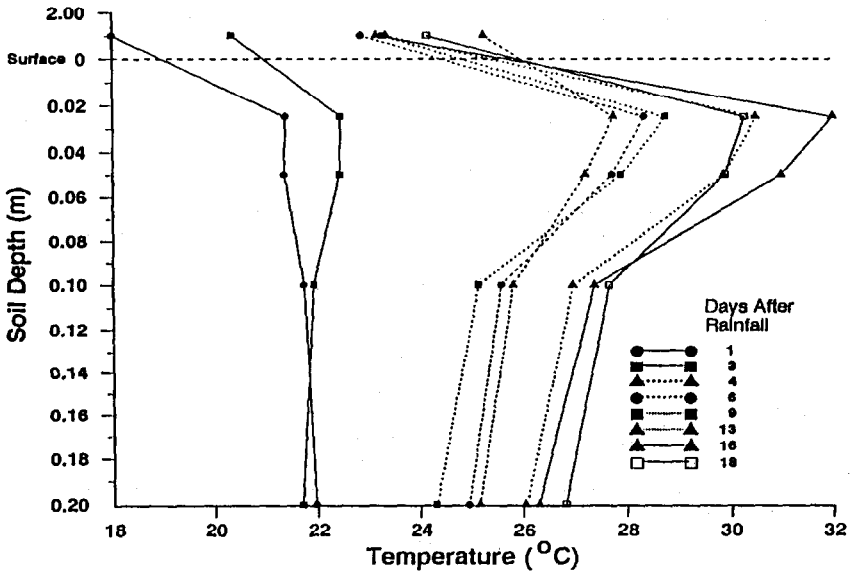

Fig. 5. Profile distribution of mean soil temperature (°C) on days after a rainfall, CPER, 1988. The data points above the surface dotted lines refer to mean air temperature for the day measured at 1 m above the soil surface.

3.3. Wind speed and direction

Wind speed is an important factor in assessing surface conductance to heat and vapor flux from the soil–vegetation system to the atmosphere. The general form of wind speed profile over an extensive uniform surface under neutral atmospheric conditions is expressed as

$$u(z) = u^* k^{-1} \left[\frac{\ln(z-d)}{z_o} \right] \tag{8}$$

where $u(z)$ is the time-average wind speed ($m\,s^{-1}$) measured at height z, u^* is the friction velocity ($m\,s^{-1}$), z_o is the canopy aerodynamic roughness length, and d is the displacement height at which the above-canopy mixing length dissipates to zero (Thom, 1975). Using hourly wind speed measurements at 1, 2 and 4 m heights above the canopy taken from a total of 196 days during the 1988–1989 vegetative season and under near-neutral conditions (characterized by wind speed of $4\,m\,s^{-1}$ or more and $S_t \leq 100\,W\,m^{-2}\,h^{-1}$), d was found to be zero. z_o varied from 9.23×10^{-3} to 3.02×10^{-2} m as the grass increased in height (maximum of 0.05–0.07 m) and basal cover. The iteration procedure employed in deriving d and z_o, and limitations of this method, were described by Robinson (1962). Numerical models of air flow above and below plant canopies indicated that for sparse canopies, d reduces to zero presumably because of the lack of control of the canopy elements on the mixing length (Seginer, 1974; Kondo and

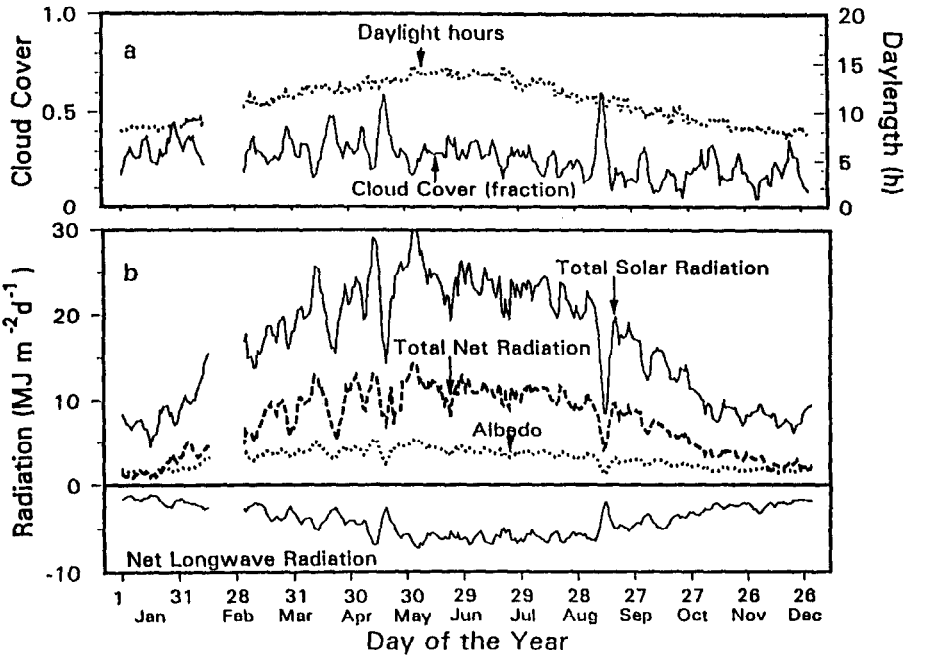

Fig. 6. Seasonal distribution of (a) daily daylight hours (h day^{-1}), fraction of cloud cover, and (b) components of the radiation balance (MJ m^{-2} day^{-1}) in the shortgrass prairie, 1986–1989. The gap in the curves between 16 February and 5 March represents missing values.

Akashi, 1976). Massman (1992) obtained a mean value of $z_o = 0.018$ m in the shortgrass steppe and noted large uncertainties in the value of z_o derived.

Wind speeds at the shortgrass steppe between May and September were fairly uniform at 4 m (3.75 ± 1.10 m s^{-1}), 2 m (3.22 ± 0.98 m s^{-1}), and 1 m (2.46 ± 0.84 m s^{-1}) above the ground surface. Gusts approaching 16 m s^{-1} or more occurred often between October and April. These strong winds come from the northwest direction, corresponding to the continental pattern of strong westerly flow between 35 and 55°N prevalent during the winter and spring months (March–May). The prevalent wind direction between the months of May and October was southeast, and was caused by the weakening of the westerlies.

3.4. Radiation receipt and partitioning of radiative energy

The seasonal distribution of daylight hours, fraction of cloud cover (F_c), and of the radiation balance components are shown in Fig. 6(a) and Fig. 6(b). Between May and October, 80% of the days were consistently clear ($F_c \leq 0.4$), with the clearest day having $F_c = 0.14$ (Fig. 6(a)). Total incoming solar radiation (S_t) showed a bell-shaped type of distribution, peaking in July with values greater than 30 MJ m^{-2} day^{-1}. The

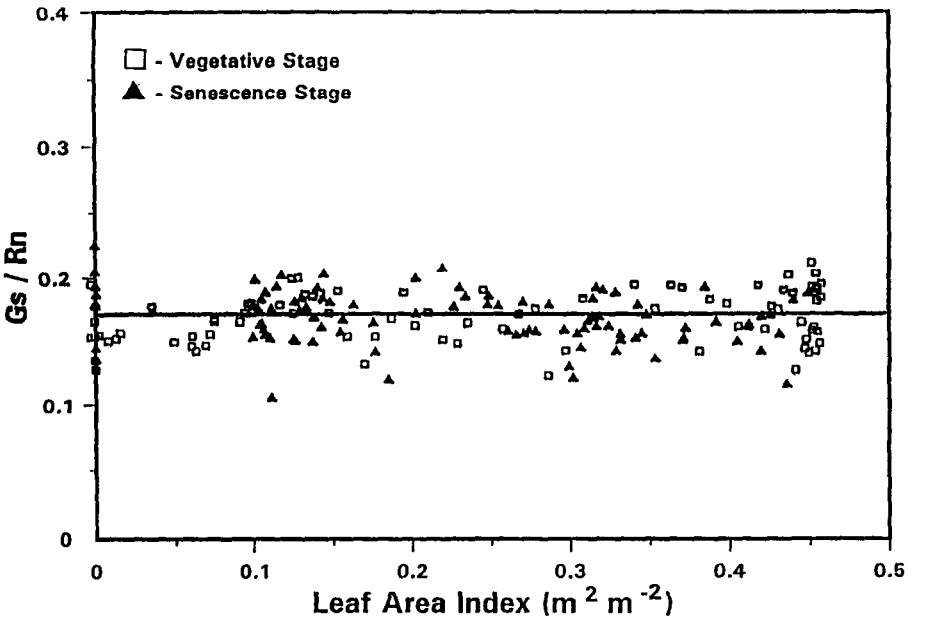

Fig. 7. Proportion of radiative energy conducted into the soil (G_s / R_n) as determined by vegetation cover, CPER, 1988.

seasonal distribution of the daily maximum solar radiation received ($S_{t(max)}$; MJ m^{-2} day^{-1}) at the shortgrass steppe ($r^2 = 0.92$, RMSE = 1.85) can be described by

$$S_{t(max)} = 9.1258 + 23.5472\sin^2\left[\frac{\pi(\text{Day} + 10)}{365}\right] \quad (9)$$

where $S_{t(max)}$ values used for fitting the equation were derived from Lagrange polynomial interpolation of the maximum data points shown in Fig. 6(b) (Johnson and Thornley, 1983). The daily total direct component of incoming solar radiation (S_d) can be obtained by multiplying $S_{t(max)}$ by $(1 - F_c)$.

Total net radiation (R_n) closely followed the distribution of solar irradiance and was estimated to be equal to 47% of S_t ($r^2 = 0.99$; RMSE = 0.68). Low R_n can be attributed to the high surface albedo (Fig. 1) and high outgoing longwave radiation associated with long periods of dry soil conditions and high soil surface temperatures at the site.

In a soil–vegetation system, the net radiant energy absorbed is partitioned to drive evapotranspiration (λE) and photosynthesis (P), with a portion dissipated into the soil (G_s) and convected into the atmosphere (H). P is relatively small compared with the other components of the surface energy and was not considered. Using daily integrated values of G_s and R_n taken during clear days ($F_c \leq 0.2$), the proportion of G_s relative to R_n remained uniformly equal to 0.167 ± 0.037 during the vegetative (April–July) and senescence (August–October) phases of the grass development (Fig. 7). This indicated that there was very little attenuation of R_n even when the maximum leaf area index (LAI = 0.5) was reached. In contrast to these results, Choudhury et al. (1987) obtained

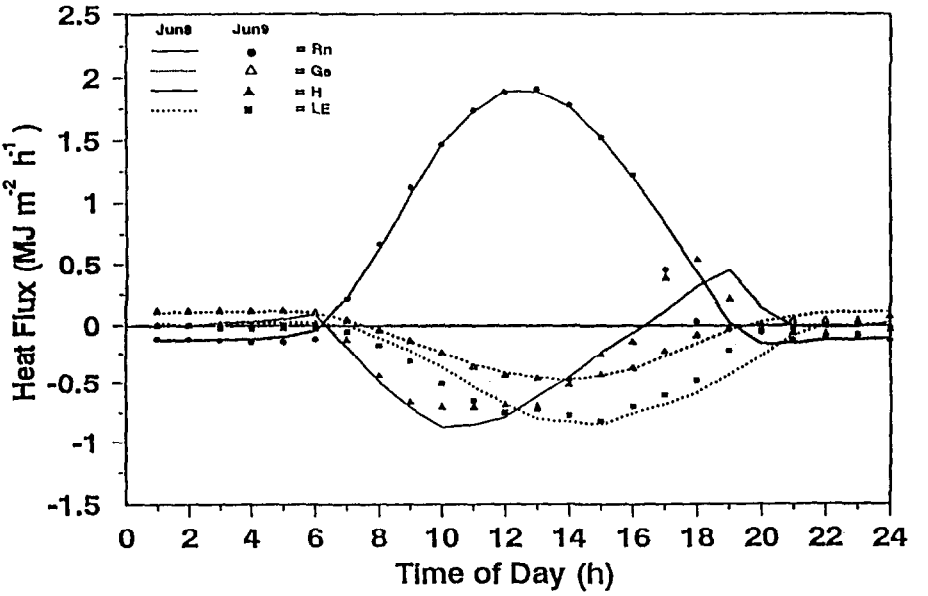

Fig. 8. Surface energy balance ($MJ\,m^{-2}\,h^{-1}$) taken on two clear days, 8 June (lines) and 9 June (symbols), CPER, 1988.

an almost linear decrease in G_s/R_n in wheat from initial development until the crop obtained complete canopy cover.

Fig. 8 shows the diurnal partitioning of radiative heat energy on two clear days ($F_c = 0.14$; LAI = 0.5) in the shortgrass steppe. Latent heat flux (λE) was derived from lysimeter measurements. Sensible heat flux (H) was obtained from the hourly difference in R_n and the sum of λE and G_s measurements. R_n peaked close to solar noon whereas G_s and λE lagged behind by half an hour to 2 h, following closely the diurnal pattern of air and soil temperatures. Sensible heat flux was greater than λE in the morning, indicating that most of the energy received at this time of the day was used to warm the air. From midday towards the end of the afternoon, R_n was increasingly partitioned into G_s and λE. The positive H observed towards the end of the day may be due to advected energy coming from the surrounding dry areas. The relatively higher λE on the morning of 9 June compared with the previous day may be due to the additional surface water formed from night-time condensation (0.02 cm). These patterns of radiant energy partitioning were consistently observed between May and October on days with clear skies that follow rainfall.

Sensible heat flux can be estimated from the ratio of the temperature difference between the surface and the air ($T_{surf} - T_a$) and the aerodynamic resistance (r_a). Because r_a is affected by atmospheric stability, wind speed, and surface roughness (Hatfield et al., 1983), the complications in estimating H associated with deriving r_a can be alleviated by establishing a proportionality between H and ($T_{surf} - T_a$). Previous studies indicated that instantaneous H at midday can be estimated from a simple relationship

Table 2
Correlation coefficients [a] between sensible heat flux (H), Bowen ratio (β), and temperature differences between the plant canopy and the air ($T_{can} - T_{air}$) and soil temperature taken at 0.025 m depth and the air ($T_{soil} - T_{air}$)

Variables	β	$T_{can} - T_{air}$	$T_{soil} - T_{air}$
H	0.96	0.69	0.94
β		0.66	0.88

[a] Correlations are significant at $P \leq 0.01$.

with $(T_{surf} - T_a)$ taken at midday (Jackson et al., 1977; Seguin and Itier, 1983; Brunel, 1989). Generally, T_{surf} is the plant canopy or surface soil temperature measured using hand-held or air-borne infrared (IR) thermometers and T_a is taken from nearby meteorological station measurements.

Similarly, if the proportionality between midday estimates (or measurements) of the ratio of H and R_n $[(H/R_n)_{\{12\,h\}}]$ and the ratio of daily integrated values of H and R_n $[(H/R_n)_{\{day\}}]$ can be established, ET_{day} can be obtained from Riou et al. (1988) and Brunel (1989) and expressed as

$$ET_{day} = R_{n(day)}\left[1 - \left(\frac{H}{R_n}\right)_{day} - \left(\frac{G_s}{R_n}\right)_{day}\right] \tag{10}$$

where $R_{n(day)}$ is given as $0.47S_t$.

Correlation analysis (Statistical Analysis Systems Institute, Inc., 1988) indicated a stronger dependence of H and the Bowen ratio (β) on the difference between soil temperatures taken at 0.025 m depth and the air $(T_{soil} - T_a)$ than on the plant canopy and air temperature $(T_{can} - T_a)$ difference (Table 2). The data used in the analysis were taken during the four wetting–drying events shown in Fig. 4(b) and three additional wetting–drying events in 1987 and 1989. The Bowen ratio was calculated as the ratio of H and λE. The higher correlation of H and β with $(T_{soil} - T_a)$ than with $(T_{can} - T_a)$ can be explained by the difficulty in isolating canopy temperature measurements from soil temperature, owing to the narrow leaf width, sparse grass density, and wide field of view (8°) of the hand-held IR thermometer used. Consequently, the relative contribution of the canopy elements to sensible heat flux may be masked by the higher soil temperature effects. Hence, in the succeeding calculations for ET_{day}, we used T_{soil} for T_{surf}. In effect, this procedure will determine if surface temperature measurements (hand-held, air-borne, or space-borne) made using IR thermometers are applicable in assessing ET_{day} in sparsely populated shortgrass prairie.

Using midday measurements from selected wetting–drying events in 1987 and 1988, the least-squares fit of $(H/R_n)_{\{12\,h\}}$ with $(T_{soil} - T_a)$ is shown in Fig. 9. Because of the wide scatter of data points observed on the driest phase of the wetting–drying event (ET_{day} is minimum), these data were excluded in deriving the relationship. This, in effect, sets the limit of application of the $(H/R_n)_{\{12\,h\}}$ vs. $(T_{soil} - T_a)$ relation to the wet-end and the rapid dry-down phases of the wetting–drying event. Such restriction would indicate three important points. First, the water content at and immediately below the surface greatly influenced T_{soil}. Second, the sensitivity of the $(H/R_n)_{\{12\,h\}}$ vs.

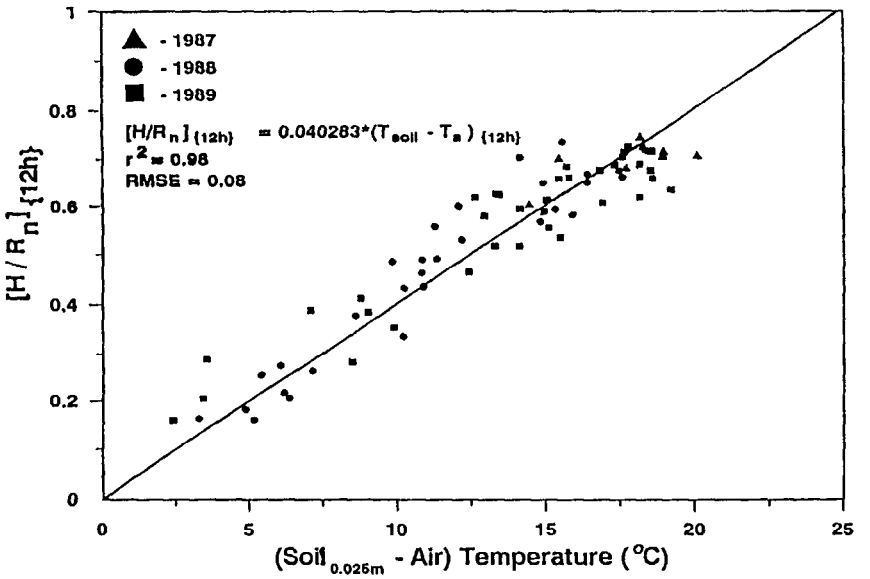

Fig. 9. Relationship between the ratio of H and R_n ($(H/R_n)_{\{12h\}}$), and the difference between soil temperature measured at 0.025 m below the soil surface and air temperature ($(T_{soil} - T_a)_{\{12h\}}$). All variables were measured at 12:00 h (MST).

$(T_{soil} - T_a)$ equation is limited to assessing the evaporation component of ET_{day}. Lastly, the high linearity in $(H/R_n)_{\{12h\}}$ vs. $(T_{soil} - T_a)$ indicates that under high soil water content, $(T_{soil} - T_a)$ may serve as a better index than $(T_{can} - T_a)$ for assessing water loss in sparse vegetation with low soil cover. Conversely, $(T_{can} - T_a)$ may be more suitable to use than $(T_{soil} - T_a)$ during the dry phase of wetting–drying events, when plant transpiration becomes the major contributor to the total evapotranspiration.

The proportionality between $(H/R_n)_{\{12h\}}$ and $(H/R_n)_{\{day\}}$ in the shortgrass prairie is shown in Fig. 10. The linear relationship has also been shown by Riou et al. (1988) for bare soils. Substituting the parameter coefficients obtained for estimating the different components of Eq. 10 gives the expression for ET_{day} (cm day^{-1}) as

$$\lambda ET_{day} = 0.1 S_t [0.3931 - 0.0174(T_{soil} - T_a)_{\{12h\}}] \quad (11)$$

where λ is the latent heat of vaporization (MJ kg^{-1} K^{-1}) described by Henderson-Sellers (1984) as a function of mean daily air temperature (T_k; K) as

$$\lambda = 1.91846 \left[\frac{T_k}{(T_k - 33.91)} \right]^2 \quad (12)$$

Evapotranspiration estimates using Eq. 11 were reasonably close to evapotranspiration values measured on 25 separate wetting–drying events in 1988 and 1989 (Fig. 11). As the soil surface dried, the amount of water loss was increasingly overestimated, owing to lack of vegetation controls (e.g. stomatal resistance) built into the equation.

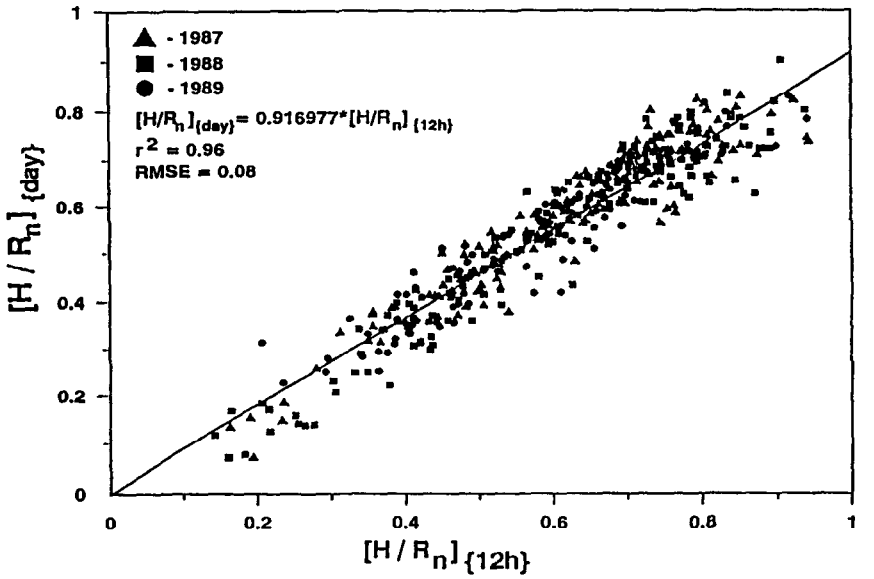

Fig. 10. Relationship between the ratio of H and R_n ($(H/R_n)_{\{12h\}}$) taken at 12:00 h (MST) and the ratio of daily integrated values of H and R_n ($(H/R_n)_{\{day\}}$).

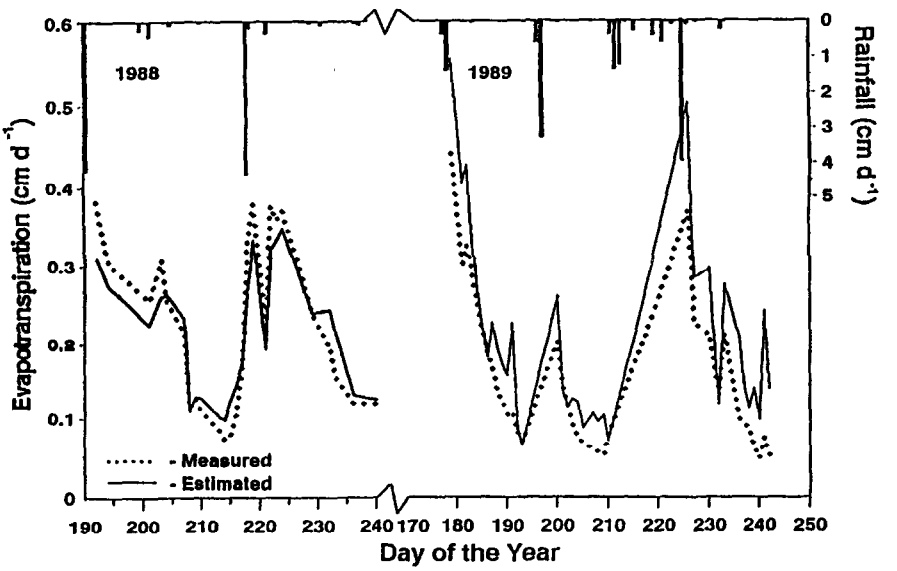

Fig. 11. Comparison between the estimated and measured evapotranspiration (cm day^{-1}) rates taken from 25 separate wetting–drying events in 1988 and 1989.

The threshold level of ET_{day}, where the evaporation of the surface soil water diminished and plant transpiration becomes the major contributor to total ET_{day}, was observed at 0.2 cm day^{-1}. Once this threshold level was reached, the error estimates of ET_{day} started to increase exponentially with further drying of the soil. The $(T_{soil} - T_a)$ difference continuously increased even when ET_{day} asymptotically approached 0.1 cm day^{-1}, resulting in 0.1–0.25 cm day^{-1} higher ET_{day} estimates.

The suitability of Eq. 11 for assessing water loss required further extensive validation. The tests made in this study were limited to the CPER site because of the lack of fully instrumented sites in the shortgrass steppe that can provide the sets of data required for the validation. Also, there were no adequate grass temperature data to provide a clearer relationship between changes in plant temperature and those of water loss in the study. The canopy temperature measurements taken in 1989 may not be a true representation of the actual grass temperature because of the masking effect of soil temperature viewed by the IR thermometer. Considering the low soil cover in the shortgrass steppe, remote radiative-temperature measurements of the grass vegetation would require soil corrections to obtain the true plant canopy temperature. Further studies that would integrate plant temperature and vegetation controls to Eq. 11 are suggested to extend the application of this method of estimating ET_{day} over a wider range of soil moisture.

4. Summary and conclusion

Although extreme fluctuations in the microclimate of a shortgrass steppe typical of a semi-arid environment are often encountered, this study showed annually consistent patterns in the seasonal distribution of the microclimatic factors. This enabled us to describe these seasonal distributions in empirical equations with a high degree of certainty. A method for describing changes in daily evapotranspiration rates during wetting–drying events was also proposed. The method uses an energy balance approach where sensible heat flux is derived from the difference in midday measurements of soil temperature at 0.025 m below the surface and air temperature. The suitability of the method for estimating daily evapotranspiration is limited to sparse vegetation with low soil cover and under conditions of high soil moisture. Further validation of the method taking into consideration the spatial heterogeneity in soil conditions at the shortgrass steppe is recommended.

Acknowledgements

We thank William Massman, Tom Kirchner, and Dave Nielsen for helpful reviews, Dave Bigelow and Susan Stokes for providing the rainfall data, and Mark Lindquist for help in data acquisition. Donald Hazlett provided plant data and insight into the development and distribution of blue grama grass in the shortgrass steppe. The use of trade and company names is for the sole benefit of the reader. No endorsement is intended by the authors and the institutions they represent.

References

Armijo, J.D., Twitchell, G.A., Burman, R.D. and Nunn, J.R., 1972. A large, undisturbed weighing lysimeter for grassland studies. Trans. ASAE, 15: 827–830.

Brunel, J.P., 1989. Estimation of sensible heat flux from measurements of surface radiative temperature and air temperature at two meters: application to determine actual transpiration rate. Agric. For. Meteorol., 46: 179–191.

Choudhury, B.J., Idso, S.B. and Reginato, R.J., 1987. Analysis of an empirical model for soil heat flux under a growing wheat crop for estimating evaporation by an infrared temperature-based energy balanced equation. Agric. For. Meteorol., 39: 283–297.

Dickinson, R.E., Henderson-Sellers, A., Kennedy, P.J. and Wilson, M.F. 1986. Biosphere–atmosphere transfer scheme (BATS) for the NCAR community climate model. NCAR/TN-275+STR, NCAR, Boulder, CO.

Dougniaux, R., 1976. Computer procedures for accurate calculation of radiation data related to solar energy utilization. Solar Energy Proc., UNESCO–WMO Symp., Geneva, Switzerland.

Hatfield, J.L., Perrier, A. and Jackson, R.D., 1983. Estimation of evaporation at one time of day using remotely sensed surface temperature. Agric. Water Manage., 7: 341–350.

Hazlett, D., 1992. Leaf area development of four plant communities in the Colorado Steppe. Am. Midl. Nat., 127: 276–289.

Henderson-Sellers, B., 1984. A new formula for latent heat of vaporization of water as a function of temperature. Q. J. R. Meteorol. Soc., 110: 1186–1190.

Jackson, R.D., Reginato, R.L. and Idso, S.B., 1977. Wheat canopy temperature: a practical tool for evaluating water requirements. Water Resour. Res., 13: 651–657.

Johnson, I.R. and Thornley., J.H.M., 1983. Vegetative crop growth model incorporating area expansion and senescence, and applied to grass. Plant Cell Environ., 6: 721–729.

Kasten, F., 1966. A new table and approximation formula for relative optical air mass. Arch. Met. Geophys. Bioklim., B14: 206.

Klipple, G.E. and Costello, D.F., 1960. Vegetation and cattle response to different intensities of grazing on shortgrass range on the central Great Plains. US Dep. Agric. Tech. Bull., 1216, 82 pp.

Kondo, J. and Akashi, S., 1976. Numerical studies on the two-dimensional flow in horizontally homogeneous canopy layer. Boundary-Layer Meteorol., 10: 255–272.

Lauenroth, W.K. and Dodd, J.L., 1978. The effect of water- and nitrogen-induced stress on plant community structure in a semiarid grassland. Oecologia, 36: 211–222.

List, R.J., 1971. Smithsonian Meteorological Tables, 6th edn. Smithsonian Institution Press, Washington, DC.

Massman, W.J., 1992. A surface energy balance method for partitioning evapotranspiration data into plant and soil components for a surface with partial canopy cover. Water Resour. Res., 28: 1723–1732.

Parton, W.J., 1984. Predicting soil temperatures in a shortgrass steppe. Soil Sci., 138: 93–101.

Parton, W.J., Schimel, D.S., Cole, C.V. and Ojima, D.S., 1987. Analysis of actors controlling soil organic matter levels in Great Plains grasslands. Soil Sci. Soc. Am. J., 51: 1173–1179.

Parton, W.J., Stewart, J.W.B. and Cole, C.V., 1988. Dynamics of C, N, P and S in grassland soils: a model. Biogeochemistry, 5: 109–131.

Riou, C., Itier, B. and Seguin, B., 1988. The influence of surface roughness on the simplified relationship between daily evaporation and surface temperature. Int. J. Remote Sens., 9: 1529–1533.

Robinson, S.M., 1962. Computing wind profile parameters. J. Atmos. Sci., 19: 189–190.

Sala, O.E. and Lauenroth, W.K., 1982. Small rainfall events: an ecological role in semiarid regions. Oecologia, 53: 301–304.

Sala, O.E. and Lauenroth, W.K., 1984. Root profile and the ecological effect of light rainshowers in arid and semi-arid regions. Am. Midl. Nat., 114: 406–408.

Schimel, D. and Parton, W.J., 1986. Microclimatic controls of nitrogen mineralization and nitrification in shortgrass steppe soils. Plant Soil, 93: 347–357.

Schimel, D., Stillwell, M.A. and Woodmansee, R.G., 1985. Biogeochemistry of C, N and P in the catena of the shortgrass steppe. Ecology, 66: 276–282.

Seginer, I., 1974. Aerodynamic roughness of vegetated surfaces. Boundary-Layer Meteorol., 5: 383–393.

Seguin, B. and Itier, B., 1983. Using midday surface temperature to estimate evaporation from satellite thermal infrared data. Int. J. Remote Sens., 4: 371–383.

Sellers, P.J., Mintz, Y., Sud, Y.C. and Dalcher, A., 1986. A simple biosphere model (SiB) for use within general circulation models. J. Atmos. Sci., 43: 505–531.

Statistical Analysis Systems Institute, Inc., 1988. SAS/StatTM User's Guide. Release 6.03. SAS Institute, Inc., Cary, NC.

Thom, A.S., 1975. Momentum, mass and heat exchange of plant communities. In: L. Monteith (Editor), Vegetation and the Atmosphere, Vol. 1. Academic Press, London, pp. 57–109.

Van Haveren, B.P. and Galbraith, A.F., 1971. Some hydrologic and physical properties of the major soil types on the Pawnee Intensive Site. US/IBP Grassland Biome Tech. Rep. 115, Colorado State University, Ft. Collins.

Walraven, R., 1978. Calculating the position of the sun. Solar Energy, 20: 393–397.